

Hopf bifurcation of a mass-spring system with LuGre friction model

Chung Ngoc Pham
Faculty of Basic Science
Hanoi University of Mining and Geology
Hanoi, Vietnam
chunghumg86@gmail.com

Hieu Nhu Nguyen
Faculty of Mechanical Engineering and Mechatronics
Phenikaa University
Hanoi, Vietnam
hieu.nguyennhu@phenikaa-uni.edu.vn

Abstract: In this study, we analyze Hopf bifurcation of a spring-mass system placed on a conveyor belt moving at constant velocity using LuGre model with the Stribeck effect. The Stribeck effect occurs when relative velocity between two surfaces is low (i.e. near-zero velocity) for which the friction force monotonically decreases as relative velocity is increasing. To check the existence of Hopf bifurcation of system motion, we use implicit algorithm criterion developed by Liu, called Liu's criterion, on the basis of the Routh-Hurwitz stability criterion, which is stated in terms of the coefficients of the characteristic equations instead of those of eigenvalues of Jacobian matrix corresponding to the system's equilibrium point. The bifurcated limit cycles can be observed in phase space of dynamical systems. We show that the system has undergone a supercritical Hopf bifurcation in an appropriate range of bifurcation parameters.

Keywords: LuGre model, Stribeck effect, stability, Hopf bifurcation.

I. INTRODUCTION

Friction phenomenon is common in nature and in engineering systems [1]. One often uses two main friction models, namely, the static friction model and dynamic friction model, to represent the behavior of systems with two or more objects in contact and moving relatively to each other [2]. For the static friction model, the friction force is a function that depends only on the relative velocity of two bodies in contact. Coulomb and viscous frictions belong to the type of static friction model [3,4]. This model is only suitable for sliding motions between two objects in contact with large enough relative velocity. For low velocity motion, the static friction model is no longer suitable because it does not capture effects associated with micro-motion of contact surfaces. Hence, dynamic friction models need to be developed. The dynamic friction model proposed by Dahl [5] describes the spring-like behavior of surface asperities of two bodies in contact. The Dahl model, however, does not capture the Stribeck effect, i.e. the effect in which the friction force decreases as the velocity increases in the near-zero low velocity domain. To overcome this shortcoming, Canudas de Wit [6] proposed a new model, called LuGre model. In this model Canudas de Wit introduced a new variable, called the internal state variable, which describes the average deflection of asperities of the contact surface.

Stick-slip motion can occur when two objects slide over each other at low relative velocity [7]. The LuGre model is used to describe this phenomenon relatively well, in which the model can capture both stick motion phase with relatively small displacement at the micro-size of asperities, and gross sliding motion on the macro scale after stick phase [6,7]. The sliding motion can lead to the instability of the equilibrium point in the problem of moving objects on the conveyor belt at low speed. For a certain system parameter domain, the transition from stable to unstable state is called bifurcation [8]. The investigation on the parameter domain in which the

bifurcation phenomenon occurs has an important meaning because it tells us the stable operating domain of the system, from which it is possible to design systems that can avoid the phenomenon of unexpected stick - slip motion.

In the framework of this paper, the authors proposed to use a relatively easy-to-use Hopf bifurcation criterion based on coefficients of the characteristic equation received from the Jacobian matrix of a linearized system in the neighborhood of the equilibrium point of the original nonlinear system with the LuGre friction model. This is the first time this bifurcation criterion has been used for the LuGre model applied to a mass - spring system moving on a conveyor belt at low relative velocity.

II. LU GRE DYNAMIC FRICTION MODEL

In order to understand the the qualitative and quantitative mechanisms of friction behavior, investigations on both theoretical and experimental aspects are necessary. It is found that body surfaces reveal very irregular structures at the microscopic scale and thus two surfaces make contact at a number of asperities. Surface asperities are assumed to be elastic and are modeled as brush bristles. When subjected to a tangential force, the bristles will deflect and behave as spring-like elastic motions with damping which give rise friction. The model of friction force is represented as follows [6]

$$\begin{aligned} F_{fr} &= \sigma_0 z + \sigma_1 \dot{z} + \sigma_2 v \\ \dot{z} &= v - \frac{\sigma_0 |v|}{g(v)} z \\ g(v) &= F_C + (F_S - F_C) \exp \left\{ - \frac{|v|}{v_s} \right\} \end{aligned} \quad (1)$$

where z is the average deflection of the bristles, called internal state variable; F_{fr} is the friction force; σ_0 is the contact stiffness; σ_1 is the damping coefficient of bristles;

Hopf bifurcation of a mass-spring system with LuGre friction model

σ_2 is the viscous friction coefficient; v is the relative velocity between two surfaces; $g(v)$ is the Stribeck function, F_c is the Coulomb friction force, F_s is the static friction force; v_s is the Stribeck velocity. The model described by Eq. (1) is known as the LuGre model [6] that exhibits the Stribeck effect, i.e. the effect that the friction force decreases as the relative velocity increases in the near-zero range. Because of the Stribeck effect, in this study, our attention is focused on the range of low-velocity with stick-slip phenomenon of a friction-induced vibrating system.

III. SYSTEM MODEL

To study the phenomenon of friction-induced vibration, we consider a mass-spring system moving in a conveyor belt at a constant speed v_b as illustrated in Fig. 1. The contact surface between the mass and belt is modeled by the LuGre friction as presented in Eq. (1). Thus, the number of independent variables in our system is two: the first is displacement variable x and the second is internal state variable z .

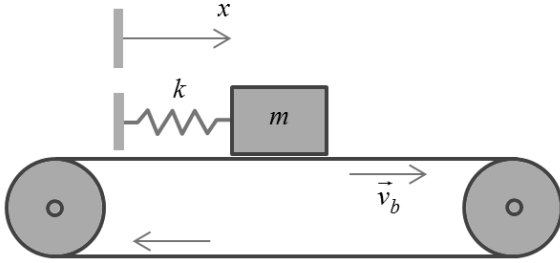


Fig. 1. A single-degree-of-freedom system placed on a conveyor belt

The governing equation of the system takes the following form:

$$\begin{aligned} m\ddot{x} &= -kx + F_{fr} \\ \dot{z} &= (v_b - \dot{x}) - \frac{\sigma_0 |v_b - \dot{x}|}{g(v_b - \dot{x})} z \end{aligned} \quad (2)$$

where m is the mass [kg], k is the spring stiffness [Nm^{-1}]. In Eq. (2), the friction force F_{fr} and the function g are determined as follows

$$\begin{aligned} F_{fr} &= \sigma_0 z + \sigma_1 \frac{dz}{dt} + \sigma_2 (v_b - \dot{x}) \\ g(v_b - \dot{x}) &= F_c + (F_s - F_c) \exp \left\{ -\frac{|v_b - \dot{x}|}{v_s} \right\} \end{aligned} \quad (3)$$

where $v_r = v_b - \dot{x}$ is relative velocity.

3.1. Equilibrium point

The equilibrium point of the system is obtained when derivatives of all system state variables in time vanishes, i.e. $\dot{x} = 0$, $\ddot{x} = 0$, $\dot{z} = 0$. This leads to the following equation for finding equilibrium point $\{x_e, z_e\}$

$$\begin{aligned} -kx_e + \sigma_0 z_e + \sigma_2 v_b &= 0 \\ v_b - \frac{\sigma_0 v_b}{g(v_b)} z_e &= 0 \end{aligned} \quad (4)$$

Solving system (4), we obtain:

$$\begin{aligned} x_e &= \frac{1}{k} [g(v_b) + \sigma_2 v_b] \\ z_e &= \frac{g(v_b)}{\sigma_0} \end{aligned} \quad (5)$$

It can be seen that the product of the deflection value of bristle at the equilibrium point of the system and stiffness coefficient σ_0 is equal to the value of the Stribeck function at the conveyor speed. The equilibrium displacement x_e is positive and depends on many factors such as the stiffness of spring k , the belt velocity v_b .

The equilibrium point in Eq. (5) can be stable or unstable depending on the determination range of system parameters. In the following subsection, the Routh-Hurwitz criterion is used to examine the stability of the equilibrium point.

3.2. Stability of equilibrium point via Routh-Hurwitz criterion

Eq. (2) can be rewritten as a system of the first-order derivative with three equations of state variables x, y, z :

$$\begin{aligned} \dot{x} &= Q_1(x, y, z) := y \\ \dot{y} &= Q_2(x, y, z) := -\frac{k}{m}x + \frac{\sigma_0}{m}z \\ &\quad + \frac{\sigma_1}{m} \left[(v_b - y) - \frac{\sigma_0 |v_b - y|}{g(v_b - y)} z \right] + \frac{\sigma_2}{m} (v_b - y) \\ \dot{z} &= Q_3(x, y, z) := (v_b - y) - \frac{\sigma_0 |v_b - y|}{g(v_b - y)} z \end{aligned} \quad (6)$$

where $Q_j = Q_j(x, y, z)$ ($j=1,2,3$) are nonlinear functions of state vector variable $\mathbf{w} = [x \ y \ z]^T$. To analyze the stability of the system (6), it is linearized in neighborhood of the equilibrium point of state vector variable, i.e. the point $\mathbf{w}_e = [x_e \ 0 \ z_e]^T$. Denote $\tilde{x} = x - x_e$, $\tilde{y} = y - 0$, $\tilde{z} = z - z_e$ as disturbance elements of state vector around the equilibrium point \mathbf{w}_e . The linearized equation system takes the following form

$$\dot{\tilde{\mathbf{w}}}_e = \mathbf{J}(\mathbf{w}_e) \tilde{\mathbf{w}} \quad (7)$$

where $\mathbf{J}(\mathbf{w}_e)$ is the Jacobian matrix of nonlinear vector $\mathbf{Q} = [Q_1 \ Q_2 \ Q_3]^T$ calculated at the point \mathbf{w}_e :

$$\mathbf{J}(\mathbf{w}_e) = \begin{bmatrix} 0 & 1 & 0 \\ j_{21} & j_{22} & j_{23} \\ 0 & j_{32} & j_{33} \end{bmatrix} \quad (8)$$

where 5 elements of the matrix \mathbf{J} are displayed in which they contain system parameters, other elements are either equal to zero or one:

$$\begin{aligned} j_{21} &= -\frac{k}{m}, j_{22} = -\frac{\sigma_2}{m} + \frac{\sigma_1}{m} h(v_b) g'(v_b) \\ j_{23} &= \frac{\sigma_0}{m} - \frac{\sigma_0 \sigma_1}{m} h(v_b) \\ j_{32} &= h(v_b) g'(v_b), j_{33} = -\sigma_0 h(v_b) \end{aligned} \quad (9)$$

in which

$$h(v_b) = v_b / g(v_b), \quad g'(v_b) = \frac{F_s - F_c}{v_s} \exp\left\{-\frac{v_b}{v_s}\right\}$$

The characteristic polynomial of the matrix (8) is found to be:

$$\lambda^3 + l_2 \lambda^2 + l_1 \lambda + l_0 = 0 \quad (10)$$

where coefficients l_2, l_1, l_0 are determined as follows

$$\begin{aligned} l_2 &= -j_{22} - j_{33} \\ l_1 &= -j_{21} + j_{22} j_{33} - j_{23} j_{32}, \\ l_0 &= j_{21} j_{33} \end{aligned} \quad (11)$$

Substituting elements j_{rs} from Eqs. (9) into Eqs. (11), we obtain

$$\begin{aligned} l_2 &= \frac{\sigma_0 v_s}{F_c} \frac{\xi}{1 + \mu_c \exp\{-\xi\}} \left[1 - \frac{\sigma_1 \mu_c F_c}{m \sigma_0 v_s} \exp\{-\xi\} \right] + \frac{\sigma_2}{m} \\ l_1 &= \frac{k}{m} \left\{ 1 + \frac{\sigma_0}{k} \frac{\sigma_2 v_s}{F_c} \frac{\xi}{1 + \mu_c \exp\{-\xi\}} \right. \\ &\quad \left. \times \left[1 - \frac{F_c}{\sigma_2 v_s} \mu_c \exp\{-\xi\} \right] \right\} \\ l_0 &= \frac{k^2}{m \sigma_2} \frac{\sigma_0}{k} \frac{\sigma_2 v_s}{F_c} \frac{\xi}{1 + \mu_c \exp\{-\xi\}} \end{aligned} \quad (12)$$

where $\xi = v_b / v_s$ is the ratio of belt velocity to Stribeck velocity; μ_c is the ratio of difference between the static and Coulomb friction forces to Coulomb friction $\mu_c = (F_s - F_c) / F_c$. Because the static friction force is larger than the Coulomb friction, the value of ratio μ_c is larger than zero, i.e. $\mu_c > 0$.

The stability condition of the system according to the Routh-Hurwitz criterion is

$$\begin{aligned} \varsigma_1 &= l_0 > 0, \\ \varsigma_2 &= l_2 > 0, \\ \varsigma_3 &= l_1 l_2 - l_0 > 0. \end{aligned} \quad (13)$$

We assume that the magnitude of parameter σ_0 is enough large such that the inequality $1 - \frac{\sigma_1 \mu_c F_c}{m \sigma_0 v_s} \exp\{-\xi\} > 0$ holds. From that, we have $l_2 > 0$. The stability condition of equilibrium point of the system is

now dependent on the third condition in (13), i.e. $l_1 l_2 - l_0 > 0$. This condition will be checked numerically in the Section 4.

3.3. Hopf bifurcation

A Hopf bifurcation gives the information on the appearance or disappearance of a periodic orbit through a local change in the stability properties of a fixed point of nonlinear dynamical systems [9]. In the traditional approach, the analysis on Hopf bifurcation is based on eigenvalues of Jacobian matrix in which a pair of complex conjugate eigenvalues will pass through the imaginary axis while all other eigenvalues have negative real parts. In case that the eigenvalues are found explicitly, this approach is convenient because we can evaluate the sign of all eigenvalues and can check the condition of Hopf bifurcation. However, the disadvantage of traditional method is that the expressions of eigenvalues may be complex if dimension of the Jacobian matrix is larger. To overcome this disadvantage, recently, Liu [10] developed a criterion on the basis of the Routh-Hurwitz stability criterion, which is stated in terms of the coefficients of the characteristic equations instead of those of eigenvalues. The Hopf analysis in our paper is based on the Liu's criterion for the system under consideration.

Applying the Liu's criterion [10] to the characteristic polynomial (10), we have the following conditions for the occurrence of Hopf bifurcation with bifurcation parameters v_b :

$$\begin{aligned} (L_1): \quad & l_0 > 0, \quad l_2 > 0, \quad l_1 l_2 - l_0 = 0 \\ (L_2): \quad & \frac{d}{dv_b} (l_1 l_2 - l_0) \neq 0 \end{aligned} \quad (14)$$

where the coefficients l_2, l_1, l_0 are determined from (12). It is noted that the condition (L_2) also can be applied to other bifurcation parameters. Two conditions $l_0 > 0, l_2 > 0$ are shown as similar to that in (13) for Routh-Hurwitz criterion. The third condition $l_1 l_2 - l_0 = 0$ in (L_1) and the condition (L_2) is checked by numerical calculation as presented in Section 4.

IV. NUMERICAL RESULTS AND DISCUSSIONS

4.1. Stable and unstable zones

Stable and unstable zones of equilibrium point in the plane of a certain pair of system parameters are formulated based on solving inequalities obtained from the Routh-Hurwitz criterion (13). Here, we are interested in two parameters: the belt velocity v_b and viscous damping coefficient σ_2 . Calculation parameters are given in Table 1. As shown before in subsection 3.2, two inequalities $l_0 > 0, l_2 > 0$ in (13) are satisfied with appropriate assumptions. Fig. 2 illustrated the graph of $\varsigma_2 = l_2$ with parameter values used in our simulations various values of belt velocity v_b from v_s to $3v_s$ with step $v_s / 10$. It is seen that values of ς_2 are all positive, therefore the condition $\varsigma_2 = l_2 > 0$ is satisfied. The inequalities $l_1 l_2 - l_0 > 0$ are also checked by numerical calculations for various values of system parameters.

Hopf bifurcation of a mass-spring system with LuGre friction model

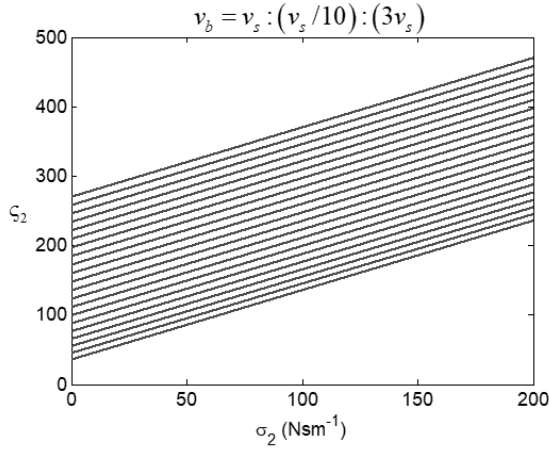


Fig. 2. Plots of curve ζ_2 as function of the viscous damping coefficient σ_2 with various values of belt velocity v_b

Fig. 3 exhibits the behavior of function $\zeta_3 = \zeta_3(v_b, \sigma_2)$ as functions of the viscous damping coefficient σ_2 with various values of belt velocity v_b from v_s to $3v_s$ with step $v_s/10$. The function ζ_3 is positive if v_b is larger than a value $v_{b,ZP}$ that is a zero-point of Eq. $\zeta_3 = \zeta_3(v_b, \sigma_2) = 0$. The solution $v_{b,ZP}$ is obtained using the Newton-Raphson method for Eq. $\zeta_3 = \zeta_3(v_b, \sigma_2) = 0$. The equilibrium point is stable if the belt velocity v_b is on the range $v_b > v_{b,ZP}$. In the following, the value $v_{b,ZP}$ is called the boundary velocity.

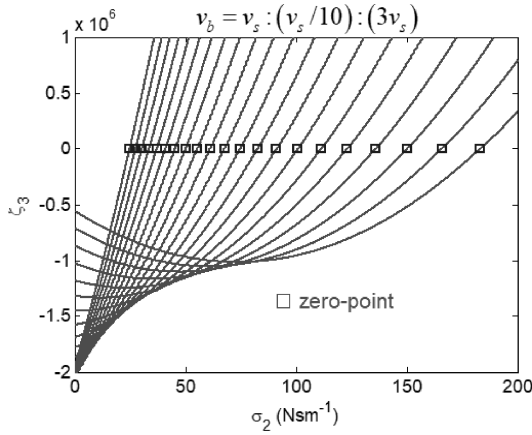


Fig.3. Plots of curve ζ_3 as function of the viscous damping coefficient σ_2 with various values of belt velocity v_b

Fig. 4 displays the graph of zero-points in Fig.3. The curve of zero-point $v_{b,ZP}$ versus the damping coefficient σ_2 illustrates a boundary of stable zone (I) and unstable zone (II) for LuGre model. The increase of viscous damping leads to a result in which the boundary velocity $v_{b,ZP}$ will be pulled down to a lower level. That means the stable state can be reached at low velocity and large damping.

TABLE 1. PARAMETER VALUES USED IN OUR SIMULATIONS

Description/Unit	Notation	Value
Mass (kg)	m	1
Spring stiffness (Nsm^{-1})	k	100
Internal stiffness (Nsm^{-1})	σ_0	10^5
Internal damping (Nsm^{-1})	σ_1	$\sqrt{10^5}$
Viscous damping (Nsm^{-1})	σ_2	0.4
Coulomb friction (N)	F_C	1
Static Friction (N)	F_S	1.5
Stribeck velocity (sm^{-1})	v_s	0.001

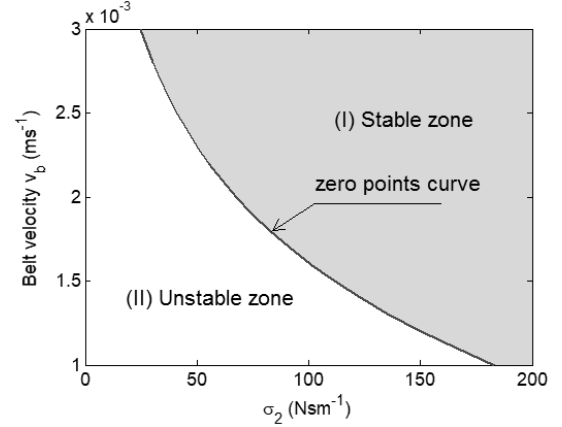


Fig. 4. Plot of zero-point curve of the function ζ_3 versus the viscous damping coefficient σ_2 . The stable zone (I) and unstable zone (II) are separated by the zero-point curve.

4.2. Hopf bifurcation analysis

The zero-point curve in Fig. 4 is obtained from the equation $l_1 l_2 - l_0 = 0$ of Hopf condition of bifurcation. If a point belonging to the stable zone (I) crosses the boundary curve, the stability of our system about the equilibrium point will change, i.e. the instability appears. To see the Hopf bifurcation, we select three points in the plane (σ_2 , v_b) in Fig. 4: S_1 (100, 1.75×10^{-3}), S_2 (86.76, 1.75×10^{-3}) and S_3 (50, 1.75×10^{-3}). The point S_1 belongs to the stable zone, the point S_2 lies on the boundary curve and S_3 drops on the unstable zone. The simulation results for phase trajectory corresponding to three points S_1 , S_2 , S_3 are portrayed on Figs. 5, 6, and 7. In Fig. 5, the phase trajectory starting from a given initial point $x(0) = 0.01$, $y(0) = v_b$, $z(0) = 1.1 \times 10^{-5}$ will approaches to the equilibrium point w_e . Here, to see the asymptotically stable property of trajectory, we choose the phase plane is $(x - x_e, \dot{x})$ instead of (x, \dot{x}) . This asymptotic behavior of phase trajectory shows that the selection of points belonging the stable zone will lead to the suppression of the system vibration. Fig. 6 exhibits a limit cycle of phase trajectory when the point S_2 lies on the boundary curve. A limit cycle is also observed in

Fig. 7 when the phase trajectory corresponding to the point S_3 is obtained after a long enough time.

In order to verify the result of Hopf bifurcation obtained from the zero-point curve, we select $v_b = 1.75 \times 10^{-3}$ and explore the behavior of eigenvalues of Jacobian matrix (8) by solving numerically the characteristic equation (10) versus the parameter σ_2 . Because Eq. (10) is a cubic polynomial form, it has a total of three solutions including imaginary ones. Each solution of Eq. 10 is separated into two parts, a real part and an imaginary part. The sign of the obtained solution will decide the stability of the system. If all real parts of solutions are negative, the equilibrium point is stable. If at least a solution with positive real part, the equilibrium point is unstable. If all solutions have negative real parts except a pair of solutions with complex conjugate pure imaginary parts, a Hopf bifurcation occurs. Figs. 8 and 9 illustrate the real and imaginary parts of eigenvalues $\lambda_1, \lambda_2, \lambda_3$ of Eq. 10 as functions of parameter σ_2 . In Fig. 8, starting from the point remarked by a squared shape, $\sigma_2 = 86.76$, the real parts of λ_2, λ_3 begin to receive negative values whereas the real part of λ_1 is always below the zero value. It is noted that the found value $\sigma_2 = 86.76$ associated with the considered value of belt velocity $v_b = 1.75 \times 10^{-3}$ is a Hopf bifurcation point. This result is the same as using the Liu's criterion (14).

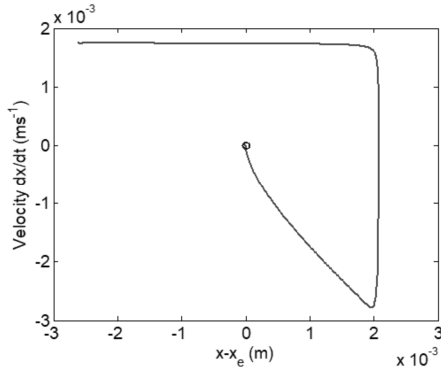


Fig. 5. Phase trajectory with belt velocity $v_b = 1.75 \times 10^{-3}$ and viscous damping $\sigma_2 = 100$

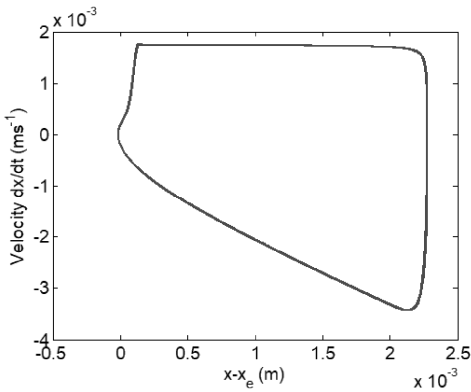


Fig. 6. Phase trajectory with belt velocity $v_b = 1.75 \times 10^{-3}$ and viscous damping $\sigma_2 = 86.76$

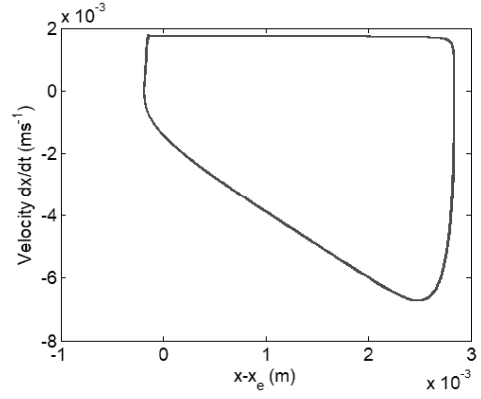


Fig. 7. Phase trajectory with belt velocity $v_b = 1.75 \times 10^{-3}$ and viscous damping $\sigma_2 = 50$

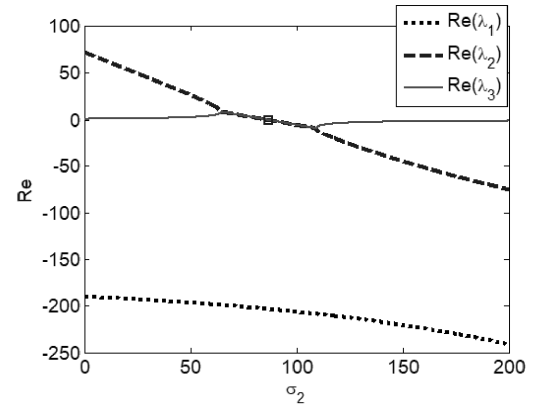


Fig. 8. Plots of real parts of eigenvalues $\lambda_1, \lambda_2, \lambda_3$ versus the parameter σ_2

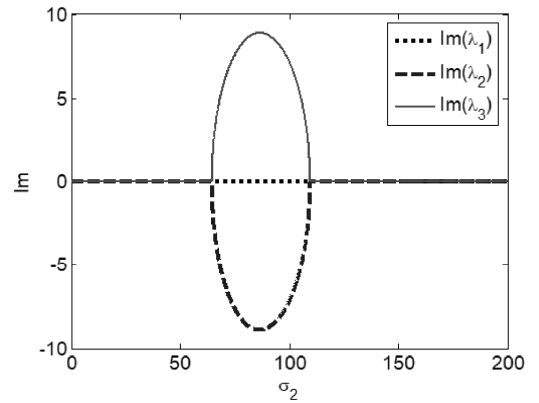


Fig. 9. Plots of imaginary parts of eigenvalues $\lambda_1, \lambda_2, \lambda_3$ versus the parameter σ_2

5. CONCLUSIONS

In the current study, using the Liu's criterion, the authors have performed a Hopf bifurcation analysis for a mass-spring system moving on the conveyor belt with constant belt velocity in low velocity domain. Stick-slip phenomenon is observed through the Hopf bifurcation. If belt velocity falls on the boundary curve, the motion state of the system under consideration will change from the stable to the unstable zone. The boundary curve shows that, in the low velocity domain, the stability of equilibrium point can be achieved by increasing value of viscous damping. In the case of higher

Hopf bifurcation of a mass-spring system with LuGre friction model

belt velocity, a stable level of equilibrium point can be attained with low viscous damping coefficient provided that damping coefficient value falls in the stable zone. The approach using Liu's criterion to find Hopf bifurcation has an advantage in comparison with the traditional approach, that is, it only uses the coefficient information of the characteristic equation instead of finding explicit solutions. Therefore, this study contributes to the understanding of the bifurcation of stick - slip motion systems in the low-velocity domain in a simpler way than the traditional approach.

REFERENCES

- [1] Brian, A.H. (1991), *Control of Machines with Friction*, Springer Science+Business Media, New York.
- [2] Guran, A., Pfeiffer, F., Popp, K. (2001), *Series on stability Dynamics with Friction: Modeling, Analysis and Experiment*, World Scientific Publishing Company Pte Limited.
- [3] Niranjan, P., Karinka, S., Sairam, K. (2017), Friction modeling in servo machines: a review. *International Journal of Dynamics and Control*, 6, pp. 893-906.
- [4] Liang, J.W., Feeny B.F. (1998), Identifying coulomb and viscous friction from free-vibration decrements. *Nonlinear Dynamics*, 16, pp. 337–47. doi:10.1023/A:1008213814102
- [5] Dahl, P.R. (1968), A solid friction model. Tech. rep.. Los Angeles, CA (USA): Space and Missile Systems Organization, Air Force System Command, ADA041920
- [6] Canudas de Wit, C., Olsson, H., Åström, K.J., Lischinsky, P. (1995), A new model for control of systems with friction. *IEEE Transactions on Automatic Control*, 40, pp. 419–425.
- [7] Pikunov, D., Stefanski, A. (2019), Numerical analysis of the friction-induced oscillator of Duffing's type with modified LuGre friction model. *Journal of Sound and Vibration*, 440, pp. 23-33, DOI: 10.1016/j.jsv.2018.10.003
- [8] Stender, M., Hoffmann, N., Papangelo, A. (2020), The basin stability of bistable friction-excited oscillators. *Lubricants*, 8, pp. 105, doi:10.3390/lubricants8120105
- [9] Hassard, B.D., Kazarinoff, N.D., Wan, Y.H. (1980), *Theory and Applications of the Hopf Bifurcation*. Cambridge: Cambridge University Press.
- [10] Liu, W.M. (1994), Criterion of hopf bifurcations without using eigenvalues. *Journal of Mathematical Analysis and Applications*, 182, pp. 250–256.